1976

Impact Fatigue of Valve Steel

M. Svenzon

IMPACT FATIGUE OF VALVE STEEL

Martin Svenzon
Steel Research Centre
Sandvik AB, Fack
S-811 01 Sandviken 1, Sweden

INTRODUCTION

Compressor valves are subjected to two types of fatigue loading, viz. bending fatigue and impact fatigue.

Bending fatigue implies manageable problems for the following reasons: easy to test in commercially available fatigue testing machines, steels with high bending fatigue limits are available and bending fatigue failure may be avoided by designing the valves so that the bending stresses are minimized.

Impact fatigue of valves is caused by repeated impacts against the seat and characterized by the tearing off of chips from the edges. Impact fatigue is more difficult to control, for many reasons. The phenomenon is not so well known as bending fatigue. Impact fatigue testing machines are not commercially available. To some extent, experimental work may be carried out in compressors but the disadvantages are obvious. It is difficult to measure the impact intensity inside a compressor and the testing is slow. There are only limited possibilities to vary the impact intensity.

TESTING

A special testing device has been developed - Sandvik Impact Fatigue Tester, SIFT. The specimen is similar to a reed valve and is set in motion by short duration compressed air pulses. The specimen thickness generally is 0.381 mm (.015") which is a standard thickness for valve steel. The shape of the specimen and seat is presented in figure 1. The specimen is clamped in the specimen holder. The cantilever part of the specimen is 50 mm.

The specimens are blanked out longitudinally in relation to the strip and are ground to the correct dimensions and shape. Finally their edges are hand polished, especially at the semicircular end, so as to give an evenly rounded edge and to eliminate any grinding marks. Normally no preparation of the surfaces of the specimens is done.

In order to generate short duration compressed air pulses a rapid valve is needed. In an ordinary valve the speed is limited by the inertial forces of the mechanical components. The rapidity can be improved by using a valve with no moving parts. This can be achieved with a fluidic device. A fluidic device is in general simply a block of solid material with an internal network of channels for the passage of air or some other fluid. The dynamic phenomena in fluidic devices are based upon the raction of a fluid jet to a confining wall. This is known as the wall attachment or Coanda effect. The wall effect fluidic device in figure 2 is based on this principle. The jet can only be made to attach itself to the other wall by breaking the vacuum between the jet and the wall. By applying air pressure at the control nozzle C_1, the jet is diverted from output B_1 to B_2. Closing control C_1, keeping C_2 open, makes the jet come out through B_1. The repeated applying and removal of the control pressure at C_1 makes the jet oscillate between B_1 and B_2. This can be achieved by a rotating slotted disk and a compressed air supply. Two pressure regulators are used for the main air and the control pressure. A filter and a magnetic valve are also parts in the compressed air system, figure 3.

The testing frequency is 250 Hz corresponding to the resonance frequency of the specimen for transverse vibrations.

The impact intensity when the specimens hits the seat can be varied continuously and measured by means of a piezoelectric accelerometer and an Impulse Precision Sound Level Meter. The impact intensity level, a, is the accelerometer signal multiplied by 10^{-3}. Unit of the accelerometer signal is m/s^2. For convenience no unit for the impact intensity level is specified here.

When a chip is torn away from the edge of the specimen due to impact fatigue, the machine is stopped by an optical fracture detector. The number of cycles to fracture is recorded.

S-N CURVES

Two standard valve steels SANDVIK 20C and SANDVIK 7C27Mo2 have been tested in SIFT. SANDVIK 20C is a carbon steel and SANDVIK 7C27Mo2 is a stainless chromium-molybdenum steel. The tensile strength of both steels was 1860 N/mm^2 (270 000 psi). The result is presented in figures 4-5. Runouts are specimens that have not

fractured when the fatigue test is deliberately discontinued and are marked with open symbols. The result has been treated statistically and S-N curves corresponding to 10 and 50% probability of fracture have been calculated.

Considering the general shape of the S-N curves it is evident that the curves level off at approximately 10^7 cycles. It can be concluded that these steels show fatigue limits when they are subjected to repeated impacts. It can also be concluded that 10^7 cycles is a proper criterion of runout for this type of loading.

Comparing SANDVIK 20C and 7C27Mo2 with reference to impact fatigue strength it is evident that SANDVIK 7C27Mo2 is superior to 20C. This is in accordance with practical experience for these valve steels.

INFLUENCE OF MATERIAL AND TESTING PARAMETERS

Composition

Impact fatigue testing of eight different strip steels has been performed in SIFT. The chemical compositions of the steels are presented in table 1. The steels A, D and F are included as they are the standard valve steel grades manufactured by Sandvik. All steels A-G have been tested in the hardened and tempered condition. The tempering temperatures have been chosen to give approximately the same tensile strength, 1860 N/mm^2 (270 000 psi). Steel H is a metastable austenitic stainless steel and has been tested in the cold rolled and tempered condition, tensile strength 1660 N/mm^2 (240 000 psi).

Fatigue testing has been performed according to the staircase method and the results have been treated statistically (30 specimens). The fatigue limit, a_f, is the impact intensity level at which 50% of the specimens can withstand 10^7 cycles. The result of the fatigue testing is shown in table 2. There is a considerable range for the fatigue limit, the highest being $a_f = 1.6$, and the lowest $a_f = 1.0$. The standard deviation is 0.3. Test of significance shows that the steels can be divided into two groups with respect to impact fatigue strength: A-C and D-H. The impact fatigue limits of the steels A-C are significantly (95% confidence level) superior to those of the steels D-H. Thus, the stainless chromium valve steel, A, belongs to the group with high impact fatigue strength and the carbon valve steels, D and F, to the other group. There is no significant difference between the fatigue limits within each group.

Tensile strength

A hardened carbon steel, SANDVIK 20C (steel D), has been tempered at five different temperatures. The lowest tensile strength was 1590 N/mm^2 (230 000 psi) and the highest 2480 N/mm^2 (360 000 psi). The standard tensile strength for valve steel with the strip thickness 0.381 mm (.015") is 1860 N/mm^2 (270 000 psi). From the result of fatigue testing presented in table 3 it can be concluded that there is no significant effect of tensile strength on the impact fatigue limit within the range 1600-2500 N/mm^2 (230 000-360 000 psi).

Surface Condition

In a special series impact fatigue testing of specimens with different surface conditions has been performed. For this investigation SANDVIK 20C (steel D) with tensile strength 1860 N/mm^2 (270 000 psi) has been used. The surface conditions were: polished (as received condition),and subsequently coarse ground, shot peened, electrolytically polished and tumbled, respectively.

The result of fatigue testing in SIFT is shown in table 4. There is little difference in the fatigue limits between the as received (polished) and any other surface condition. The only significant difference is between the results for shot peened and coarse ground finishes: as expected, the shot peened finish was superior.

Temperature

SANDVIK 7C27Mo2 and 20C (steels A and D) have been tested at elevated temperature. The compressed air was run through a heat exchanger with steam on the primary and compressed air on the secondary side. The temperature of the air after passage of the heat exchanger was equal to the steam temperature, 140°C. However, when the compressed air expanded at the nozzles its temperature was reduced to 90°C. The testing temperature was therefore 90 $\pm$ 5°C. The results show that there is no significant difference between the fatigue limits at 90°C and at room temperature.

DYNAMICS OF THE SPECIMEN

The motion of the SIFT specimen has been recorded by high-speed photography during fatigue testing, 8000 frames per second. From these frames the deflection-time curves for the specimen have been evaluated. In general the dynamics of the specimen can be described by the simultaneous vibrations corresponding to the fundamental and second tones for flexural vibrations and torsional vibrations. The deflection-time curves for the tip of the specimen are characterized by plateaux caused by second tone flexural vibrations.

The impact velocity at different impact intensity levels has been evaluated, figure 6. The impact fatigue limit of valve steels is 0.8-1.6. The corresponding impact velocities are 6-9 m/s.

When analysing the high-speed photographs it was observed that the specimen does not strike the seat perfectly squarely. As a matter of fact the specimen is always more or less bent when it strikes the seat. The angle of longitudinal obliquity has been evaluated and the result is presented in figure 7. The most frequent angle is 0.5 degrees and the largest observed angle is 3.4 degrees. Also the angle between the specimen and seat in the trans-

verse direction has been determined using an electrical contact technique with a sectioned seat. The results show that the impact is always more or less oblique in all directions. The direction of obliquity varies at random around the tip of the specimen. Oblique impact is caused by high frequency flexural and torsional vibrations of the specimen.

FRACTOGRAPHY

Specimens having fractured due to impact fatigue in SIFT have been examined by light microscopy and scanning electron microscopy. It has been found that initiation of impact fatigue fracture occurs close to the surface of the SIFT-specimen. Micro cracks appear primarily on the impact side of the SIFT-specimen at a distance of 0.1-0.3 mm from the rounded edge. The location of the initiation varies at random around the tip of the specimen. Micro cracks from an early stage of the fatigue process are always radial. Examples of typical impact fatigue fractures created in SIFT are shown in figures 8-9. Also square specimens have been tested in SIFT, figure 10. The appearance of the fatigue fractures created in SIFT are very similar to impact fatigue fracture of compressor valves. Impact fatigue testing with SIFT should therefore be considered relevant. Moreover, the effect of design of specimen and seat on the fatigue resistance can be examined in SIFT.

In order to analyse the effect of obliquity on the fatigue process the direction and magnitude of the obliquity must be controlled. This can be accomplished by making fatigue tests with an oblique seat, figure 11. By rotating the seat, the direction of obliquity may be varied. The angle of impact was in this case approximately 3 degrees. The result is presented in figure 12. The arrows indicate the direction of obliquity.

Evidently the impact fatigue fracture is always located in that part of the specimen that has been in the direction of obliquity during fatigue testing. A similar experiment has been carried out with square-shaped specimens and an oblique seat. The result is the same in this case, figure 13. Normally the fatigue fracture may occur at any corner. In this case, the first chip is always torn off from that corner which is in the direction of obliquity.

It can be concluded that maximum impact stresses are created in the part of the specimen that during each cycle makes the last contact with the seat. Evidently the impact stresses depend not only on the impact velocity but also on the impact angle.

IMPACT STRESSES

Impact fatigue strength as determined by fatigue testing in SIFT has been presented in terms of impact intensity level. This level is the accelerometer signal in m/s^2 multiplied by 10^{-3}. In a preceding section impact intensity level as a function of impact velocity of the specimen has been presented, figure 6. A typical impact velocity corresponding to a rather high impact fatigue strength is 8 m/s.

Assuming colinear impact it can be shown by one-dimensional calculations that the maximum stress amplitude in a plate impacting on a seat at rest becomes -160 N/mm^2 (-23200 psi). This is a small compressive stress in relation to the tensile strength of valve steel, 1860 N/mm^2 (270000 psi). It can not possibly cause fatigue.

A two-dimensional model has been analyzed also. These calculations have been made according to the finite difference method. The geometry of the two-dimensional model is presented in figure 14. A circular plate with velocity 8 m/s impacts on a circular seat at rest. It is assumed that the impact is colinear in this case also. The dimensions of the plate and seat have been chosen to simulate the condition at the tip of the SIFT-specimen i. e. where impact fatigue fracture occurs. The element division is presented in figure 15. Maximum and minimum stresses occurring within 2 microsonds are presented in figure 16 for a number of elements in the plate. The stresses at the position where micro cracks generally have been found on the specimen (second element from the edge) are small and the direction of the highest stress is radial. Micro cracks on the SIFT-specimen are, however, always radial. Thus the calculated stresses do not explain the observed fatigue crack appearance.

It has been shown that the obliquity of impact is of fundamental importance for the creation of fatigue failure. It can thus be concluded that the shortcoming of the one- and two-dimensional calculations is due to the fact that obliquity is not considered. Attempts have been made to calculate the effect of obliquity on the impact stress state. However, these calculations failed due to numerical difficulties.

The appearance of the cracks indicate that impact fatigue may be caused by shear stresses. The direction of the observed microcracks shows that maximum shear stresses act on planes perpendicular to the edge. Shear stresses acting on planes perpendicular to a free surface are always zero at the surface ($\tau_{zt} = \tau_{tz}$). Thus maximum shear stress must be induced at a certain distance below the surface and initiation of impact fatigue fracture should occur below the surface. This is in accordance with the fractographic observations since no signs of initiation have been found on the surface of the specimen. This is also in accordance with the experimental result that the impact fatigue strength is hardly affected by the surface condition of the specimen.

DISCUSSION

From the results presented here it can be concluded that the impact fatigue limit is affected by the chemical composition of the steel. Tensile strength surface condition and temperature, on the other hand, seem to have minor effect on the impact fatigue resistance. Attempts have been made to correlate the impact fatigue strength with other material or test parameters. However, no correlation between the static mechanical properties and impact fatigue strength could be established. No microstructural changes have been observed that might explain the different impact fatigue behaviours

of the steels. This is confirmed by hardness measurements as no hardness changes have been detected.

Measurements of the damping capacity, however, indicate that there is a correlation between the damping capacity and the impact fatigue limit for the martensitic steels. This is a probable result for the following reason. It has been shown that the obliquity of the impact is of fundamental importance for the creation of impact fatigue fracture. Oblique impact is caused by high frequency flexural and torsional vibrations of the specimen. It can be expected that these vibrations are more effectively damped in the steels which show high damping capacity and the angle of obliquity will be smaller than for the other steels. This means that local, high impact stress peaks will be avoided and the measured impact fatigue limit will be higher. This is an accordance with the experimental result obtained here, figure 17, on different martensitic steels from Table 1. It must be remembered that the damping measurements so far are limited and thus the values are only approximate. The need for careful investigation of the damping characteristics is obvious.

CONCLUSIONS

1. Sandvik Impact Fatigue Tester, SIFT, is a device in which impact fatigue experiments of reed valves can be carried out under controlled conditions.

2. The appearance of impact fatigue fracture of a SIFT-specimen is very similar to the impact fatigue fracture of compressor valves. Hence impact fatigue testing with SIFT should be considered relevant.

3. There is a fatigue limit for impact fatigue loading.

4. The S-N curves level off at approximately 10^7 cycles.

5. Results from impact fatigue testing of eight different high strength steels have been presented. The tested steels can be divided into two groups with respect to impact fatigue strength. The stainless chromium valve steel, SANDVIK 7C27Mo2, belongs to the group with superior fatigue resistance.

6. No correlation between the static mechanical properties and impact fatigue strength could be established, when comparing different steels.

7. For a given steel tensile strength, surface condition and temperature seem to be of minor importance for the impact fatigue properties.

8. The damping capacity of the steels seems to have an effect on the impact fatigue limit. Steels with high damping capacity show high impact fatigue resistance.

9. The dynamics of the SIFT-specimen can be described by the superposition of the fundamental and second tones for flexural vibrations and torsional vibrations.

10. The impact of the specimen on the seat is always more or less oblique. The obliquity angle is typically 0.5-1.5 degrees and maximum 3 degrees.

11. Obliquity of the impact is of fundamental importance for the creation of impact fatigue failure.

12. Cracks are induced in the part of the specimen that during each cycle makes the last contact with the seat.

13. Micro cracks from an early stage of the fatigue process are always perpendicular to the edge of the specimen.

Table 1
Chemical composition of tested grades, wt %

Steel	SANDVIK	C	Si	Mn	P	S	Cr	Ni	Mo	V
A*	7C27Mo2	0.36	0.37	0.37	0.024	0.004	13.4	0.27	1.29	-
B	9HS74	0.48	0.24	0.78	0.013	0.005	1.12	0.54	1.0	0.10
C	7HS70	0.38	0.27	0.65	0.010	0.008	0.89	1.82	0.35	0.10
D*	20C	1.02	0.25	0.45	0.012	0.006	-	-	-	-
E	20CHV	1.02	0.24	0.40	0.008	0.007	0.18	-	-	-
F*	15M	0.76	0.27	0.72	0.009	0.011	-	-	-	-
G	13HS30	0.66	1.11	0.40	0.015	0.005	0.54	-	0.29	0.16
H	12R11	0.11	0.57	1.23	0.017	0.008	17.8	7.52	0.22	-

* SANDVIK valve steels

Table 2
Results from fatigue testing of steels with different compositions

Steel	Grade SANDVIK	Fatigue limit a_f
A	7C27Mo2	1.6
B	9HS74	1.6
C	7HS70	1.6
D	20C	1.0
E	20CHV	1.2
F	15M	1.1
G	13HS30	1.1
H	12R11	1.1

Table 3
Tensile and impact fatigue properties of SANDVIK 20C tempered at five different temperatures

Tensile strength N/mm^2	1000 psi	Fatigue limit a_f
1590	230	1.2
1870	270	1.0
2070	300	0.9
2230	325	1.0
2480	360	1.2

Table 4
Influence of surface treatment on impact fatigue resistance. Results of fatigue testing.

Surface treatment	Fatigue limit a_f
Polished	1.0
Coarse ground	0.8
Shot peened	1.2
Electrolytically polished	0.9
Tumbled	1.1

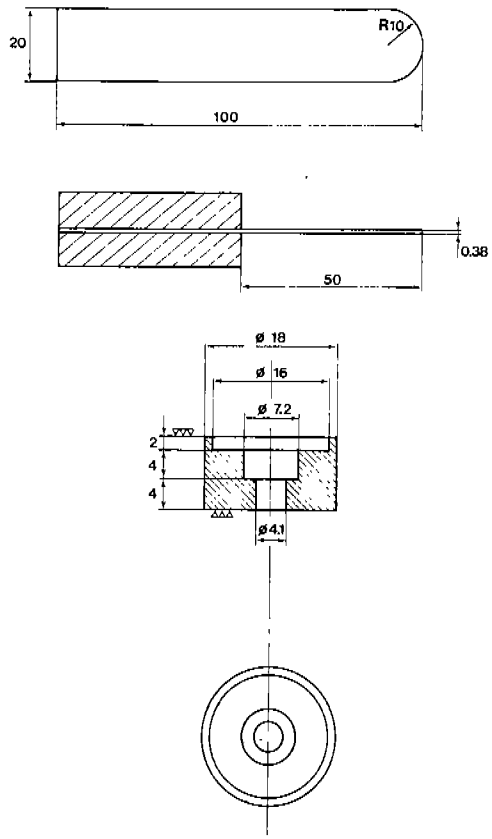

Figure 1
Specimen and seat. The material in the seat is hardened tool steel, HRC 58.

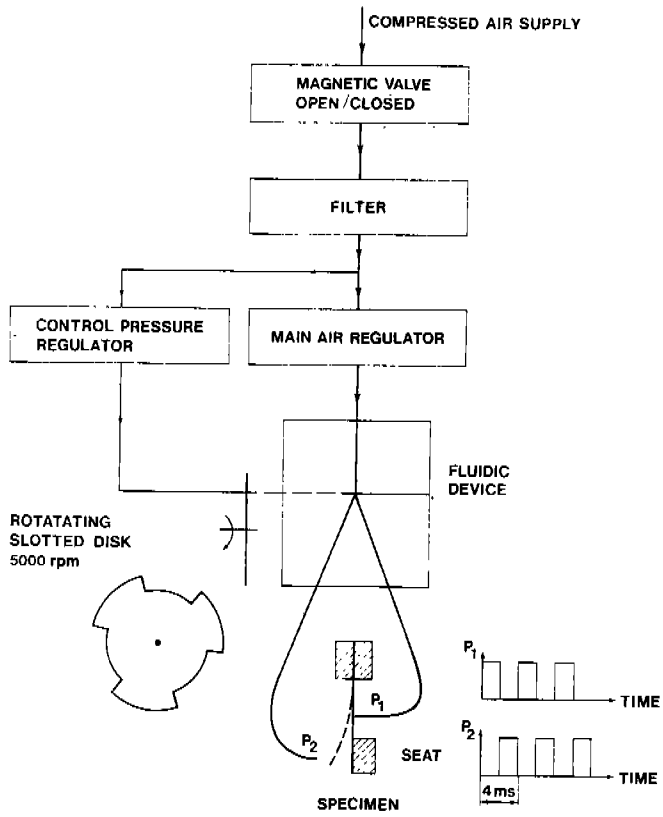

Figure 3
Compressed air system.

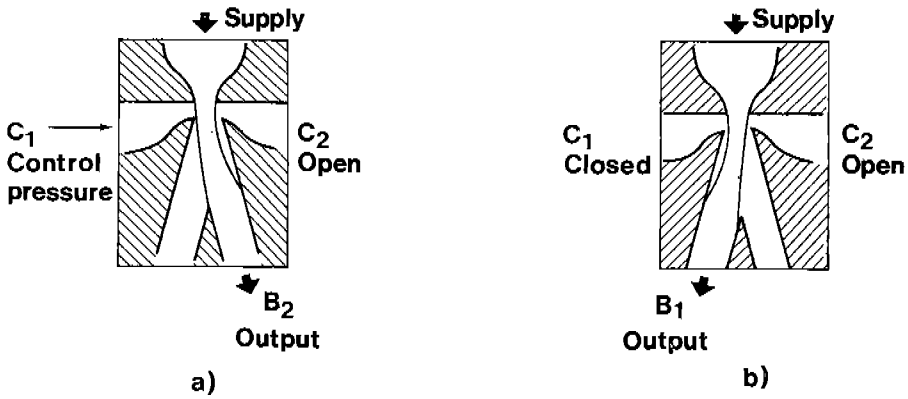

Figure 2
The bistable wall effect fluidic device. The main compressed air flow enters at A and leaves through B_1 or B_2 depending on the control pressure at C_1.
a) When the control pressure is applied at C_1 the air flow leaves through B_2
b) With C_1 closed (C_2 open) the air flow leaves through B_1

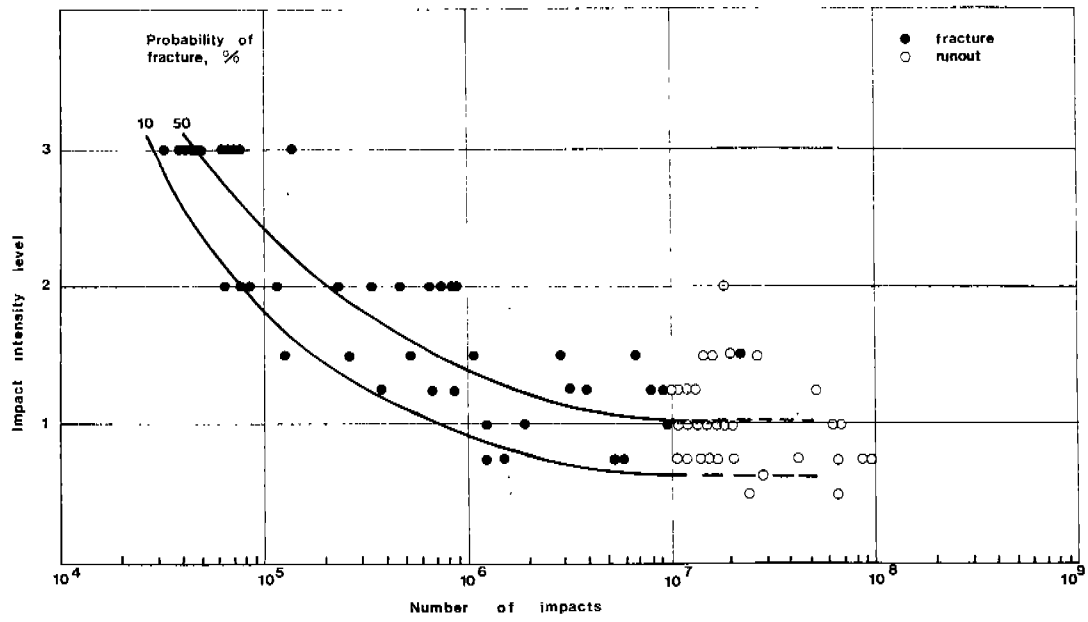

Figure 4
S-N curves for SANDVIK 20C.

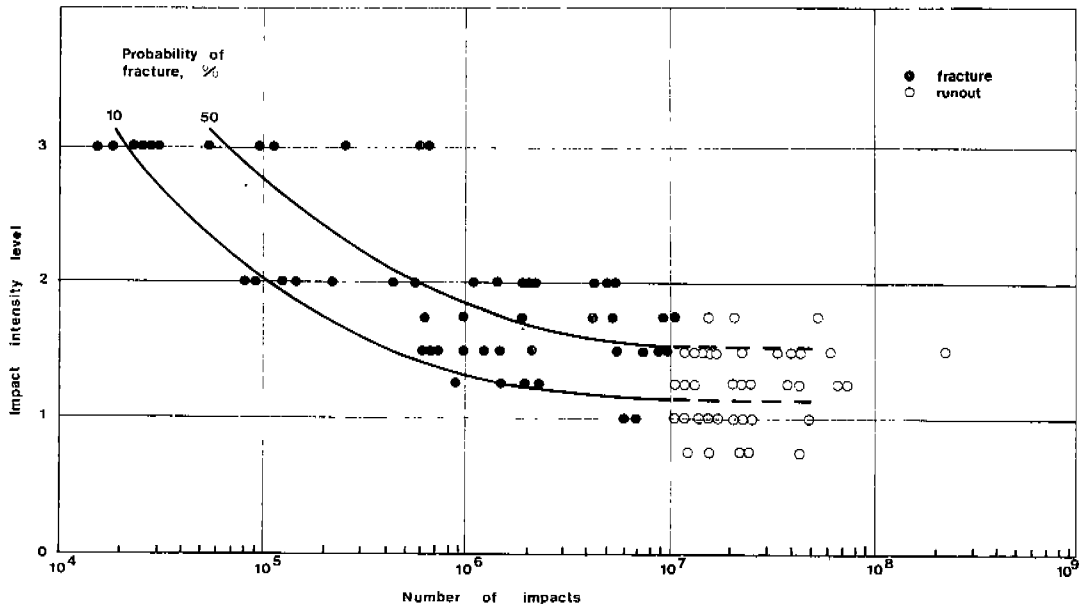

Figure 5
S-N curves for SANDVIK 7C27Mo2.

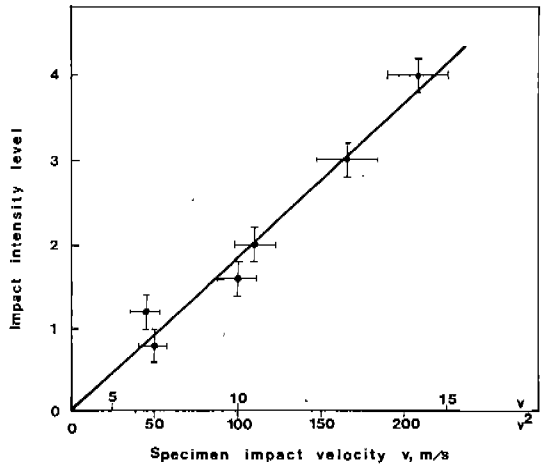

Figure 6
Impact intensity level as a function of impact velocity of the tip of the specimen.

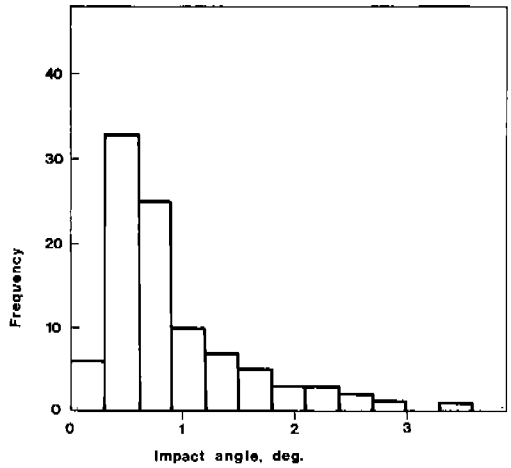

Figure 7
Histogram of longitudinal obliquity angle as measured from high-speed photographs.

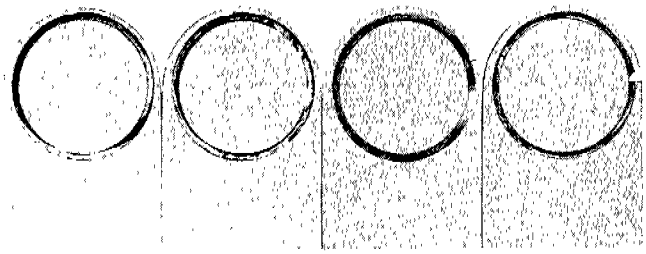

Figure 8
Early stage impact fatigue fractures.

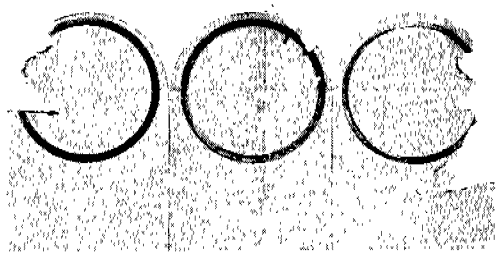

Figure 9
Late stage impact fatigue fractures.

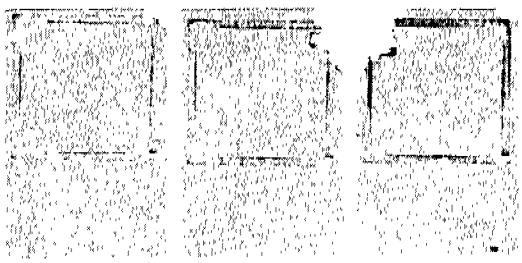

Figure 10
Impact fatigue fractures of square specimens.

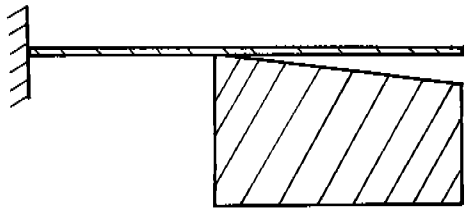

Figure 11
Oblique seat.

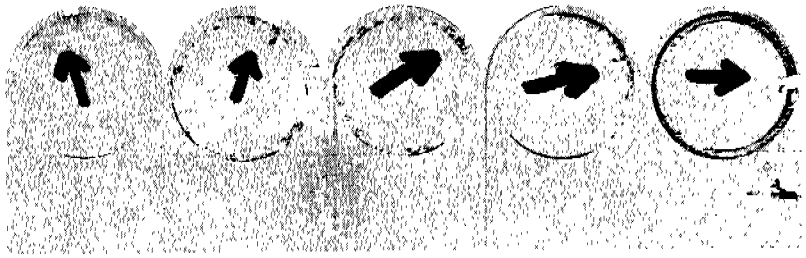

Figure 12
Standard specimens tested against an oblique seat. The arrows indicate the direction of obliquity.

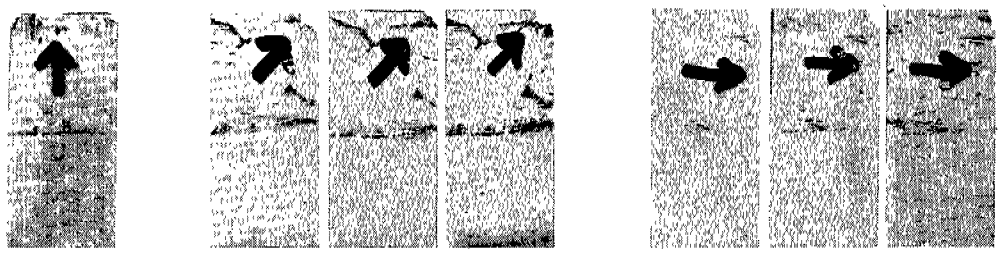

Figure 13
Square specimens tested against an oblique seat. The arrows indicate the direction of obliquity.

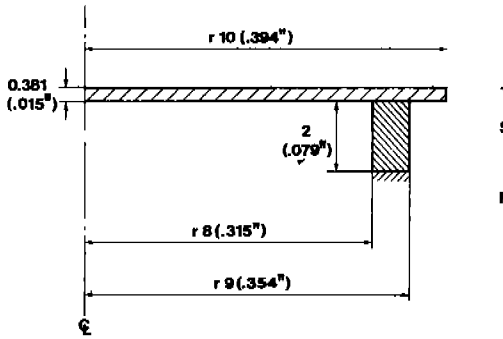

Figure 14
Circular plate and seat.

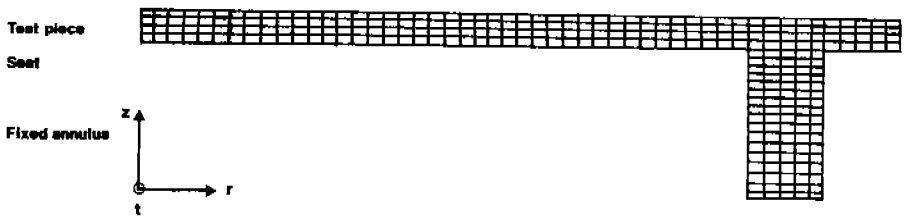

Figure 15
Element division. Element size 0.20x0.095 mm.

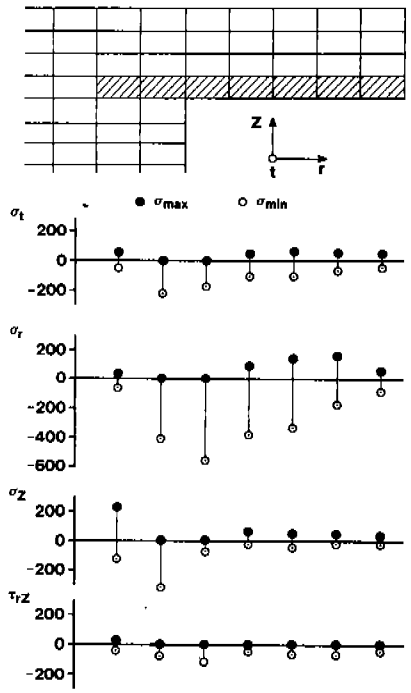

Figure 16
Maximum and minimum stresses for a number of elements in the plate.

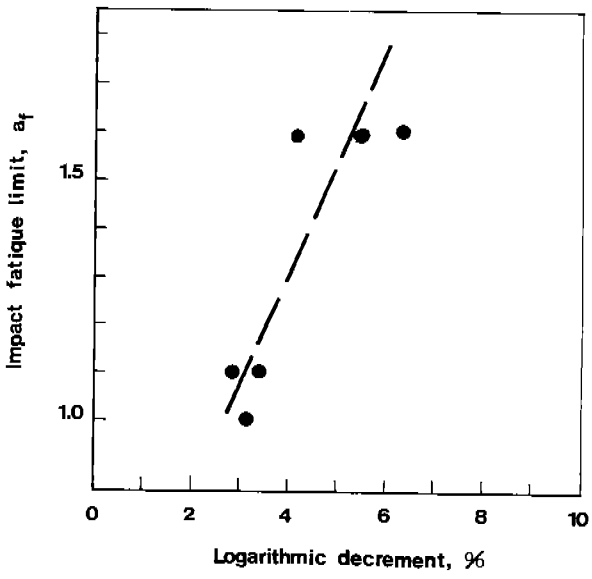

Figure 17
Impact fatigue limit versus logarithmic decrement for some martensitic steels.